

On the K^+D interaction at low energies

V. E. Tarasov, V. V. Khabarov, A. E. Kudryavtsev, V. M. Weinberg

Institute of Theoretical and Experimental Physics

Moscow, Russia

The Kd reactions are considered in the impulse approximation with NN final-state interactions (NN FSI) taken into account. The realistic parameters for the KN phase shifts are used. The "quasi-elastic" energy region, in which the elementary KN interaction is predominantly elastic, is considered. The theoretical predictions are compared with the data on the $K^+d \rightarrow K^+pn$, $K^+d \rightarrow K^0pp$, $K^+d \rightarrow K^+d$ and K^+d total cross sections. The NN FSI effect in the reaction $K^+d \rightarrow K^+pn$ has been found to be large. The predictions for the Kd cross sections are also given for slow kaons, produced from $\phi(1020)$ decays, as the functions of the isoscalar KN scattering length a_0 . These predictions can be used to extract the value of a_0 from the data.

PACS numbers: 13.75.Jz; 24.10.-i; 25.10.+s; 25.80.Nv

1 Introduction

Recent experimental indications [1] on the possible existence of the exotic $\Theta^+(1540)$ state in the K^+N system (pentaquark $\bar{s}uudd$ state) have enhanced the interest to the K^+N and K^+d interactions. Analyses of the K^+N elastic scattering [2, 3], K^+d total cross sections [4, 5] and the reaction $K^+d \rightarrow K^0pp$ [6, 7] with isospin $I = 0$ assumed for the pentaquark led to conclusion about its small width $\Gamma \leq 1$ MeV. At present time the existence of the pentaquark seems to be doubtful since it was not confirmed by a number of experiments (see the review paper by M. Danilov and R. Mizuk listed in Ref. [1]).

In connection with the Θ^+ problem the recent paper [8] introduces a new partial-wave analysis (PWA) of K^+N scattering in the momentum range $0 < p_{\text{LAB}} < 1.5$ GeV/ c and comparison of the results with previous analyses. To extract the K^+N -scattering parameters in isospin-0 channel an additional information to the data on the proton target is required. This additional data are provided by experiments on the K^+ -deuteron collisions. The recent paper [9] contains a review of existing data on the K^+d reactions in the "quasi-elastic" region $p_{\text{LAB}} < 0.8$ GeV/ c (where the elementary KN reaction is predominantly elastic and the role of the particle-production processes is negligible), i.e. on the processes $K^+d \rightarrow KNN$ and $K^+d \rightarrow K^+d$. A reasonable description of the total cross sections and differential spectra $d\sigma/d\Omega$ for outgoing kaons was obtained in the framework of the impulse approximation with the use of the Jülich model for the KN amplitude. The papers [8, 9]

also claim that the existing K^+N and K^+d data do not prove, but do not exclude the possibility of a narrow resonance Θ^+ in the $KN(I=0)$ system.

In this paper we present the calculations of the total K^+d cross sections, the cross sections of the break-up reactions $K^+d \rightarrow K^+pn, K^0pp$ and of the elastic scattering process $K^+d \rightarrow K^+d$. We restrict our consideration to the "quasi-elastic" region $p_{\text{LAB}} < 0.8 \text{ GeV}/c$ defined above. We consider only the "background" amplitudes and neglect the possible Θ^+ contribution. In our calculations we take into account the pole diagrams and s -wave final-state interaction (NN FSI) of slow nucleons in the process $Kd \rightarrow KNN$. We express the KN -scattering (and charge exchange) amplitude through the partial-wave components, including only s - and p -wave terms which are important in the region of interest. For simplicity we use the s -wave KN -scattering amplitude when calculating the NN FSI contribution. In this approximation the KN amplitude does not contain the spin-flip term and as a result the NN FSI is taken into account only in the triplet $NN(^3S_1)$ state. Thus, according to the Pauli principle, in the case under consideration NN FSI takes place only for the process $K^+d \rightarrow K^+pn$ but not for $K^+d \rightarrow K^0pp$.

Predictions will be also given for the K^+d cross sections with slow kaons as functions of the isoscalar KN -scattering length a_0 . They can be used to extract the value of a_0 from the experiments with the kaons produced from $\phi(1020)$ decays at rest. The corresponding experiments with $\phi(1020)$ mesons produced in e^+e^- -collisions may be proposed for DAΦNE machine (Frascati).

The paper is organized as follows. In Sect. 2 we give the expressions for the partial-wave KN -scattering amplitudes and illustrate the description of the data on the KN cross sections for some sets of phase-shift parameters. In Sect. 3 we write out the amplitudes for the break-up reactions $Kd \rightarrow KNN$ (pole diagrams + NN FSI) and the elastic process $K^+d \rightarrow K^+d$. In Sect. 4 our theoretical predictions for the K^+d cross sections are presented and compared with the experimental data. Sect. 5 is the Conclusion. Some necessary formulas are placed in the Appendix.

2 KN -scattering amplitude

Let us write out the isospin structure of the KN -scattering amplitude \hat{f}_{KN} and the relations between charge and isospin amplitudes. They read

$$\hat{f}_{KN} = \hat{F}_S + \hat{F}_V \boldsymbol{\tau}_K \boldsymbol{\tau}, \quad \hat{F}_S = \frac{1}{4}(3\hat{F}_1 + \hat{F}_0), \quad \hat{F}_V = \frac{1}{4}(\hat{F}_1 - \hat{F}_0), \quad (1)$$

$$\hat{f}_{K^+p} = \hat{F}_1, \quad \hat{f}_{K^+n} = \frac{1}{2}(\hat{F}_1 + \hat{F}_0), \quad \hat{f}_{K^+n \rightarrow K^0p} = \frac{1}{2}(\hat{F}_1 - \hat{F}_0),$$

where $\boldsymbol{\tau}$ ($\boldsymbol{\tau}_K$) are the isospin Pauli matrices for nucleons (kaons) and $\hat{F}_{0,1}$ ($\hat{F}_{S,V}$) are the KN amplitudes with s -channel (t -channel) isospin $I = 0, 1$. The K^+N -scattering and

charge exchange amplitudes are¹

$$\hat{f}_{K^+N \rightarrow K^+N} = \hat{F}_S + \hat{F}_V \tau_3, \quad \hat{f}_{K^+n \rightarrow K^0p} = 2\hat{F}_V \tau_+, \quad \tau_+ = \frac{1}{2}(\tau_1 + i\tau_2). \quad (2)$$

The amplitudes \hat{F}_I ($I = 0, 1$) can be written in standard form

$$\hat{F}_I = A_I + B_I(\mathbf{n}\boldsymbol{\sigma}), \quad \mathbf{n} = \frac{\mathbf{k} \times \mathbf{k}'}{|\mathbf{k} \times \mathbf{k}'|}, \quad A_I = \sum_{l=0}^{\infty} [(l+1)f_{l+}^{(I)} + lf_{l-}^{(I)}] P_l(\cos \theta),$$

$$B_I = i \sum_{l=1}^{\infty} (f_{l+}^{(I)} - f_{l-}^{(I)}) P_l^1(\cos \theta), \quad f_{l\pm}^{(I)} = \frac{\eta \exp(2i\delta) - 1}{2ik}. \quad (3)$$

Here: \mathbf{k} (\mathbf{k}') is the relative initial (final) CM momentum; $\eta \equiv \eta_{l\pm}^{(I)}$ and $\delta \equiv \delta_{l\pm}^{(I)}$ are the inelasticities ($0 \leq \eta \leq 1$) and phase shifts for s -channel isospin I , orbital momentum l and $j = l \pm \frac{1}{2}$. At $p_{\text{LAB}} < 0.8$ GeV/ c the cross sections of particle production in the KN interactions are relatively small and $\eta_{l\pm}^{(I)} \approx 1$. Hereafter, we take $\eta_{l\pm}^{(I)} \equiv 1$ and $f_{l\pm}^{(I)} = 1/(k \cot(\delta) - ik)$.

Let us compare the KN cross sections, calculated from the existing phase shifts $\delta_{l\pm}^{(I)}$, with the data. Here we use the phase shifts from Refs. [5, 8] given in the forms

$$k \cot(\delta_{l\pm}^{(I)}) = \frac{1}{a_{l\pm}^{(I)} k^{2l}} \quad (l = 0, 1) \quad [5], \quad (4)$$

$$k \cot(\delta_{l\pm}^{(I)}) = \frac{1}{a_{l\pm}^{(I)} k^{2l}} \left(1 + \sum_{i \geq 1} b_{i,l\pm}^{(I)} k^{2i} \right) \quad (l = 0, 1) \quad [8], \quad (5)$$

$$\delta_{2\pm}^{(I)} = k^5 (c_{\pm}^{(I)} + d_{\pm}^{(I)} k^2 + e_{\pm}^{(I)} k^4), \quad \delta_{3\pm}^{(I)} = k^7 f_{\pm}^{(I)} \quad [8],$$

where $a_{l\pm}^{(I)}$, $b_{i,l\pm}^{(I)}$, $c_{\pm}^{(I)}$, $d_{\pm}^{(I)}$, $e_{\pm}^{(I)}$, and $f_{\pm}^{(I)}$ are the constants. Their values were obtained [8] from PWA of K^+N scattering in the range $p_{\text{LAB}} < 1.5$ GeV/ c , using s -, p -, d -, and f -wave amplitudes (see Tables II and VI in Ref. [8]). The values $a_{l\pm}^{(I)}$ for $l = 0, 1$ (scattering lengths and volumes) from Refs. [5, 8] are given in Table.

Fig. 1 shows the total K^+p , K^+n and $K^+N(I=0)$ cross sections. The symbols represent the experimental data, taken from Refs. [10, 11, 12, 13, 14, 15, 16, 17, 18, 19, 20, 21]. Fig. 1a shows the data on the total ($\sigma_{K^+p}^t$) and elastic ($\sigma_{K^+p}^{el}$) K^+p cross sections. The curves in Figs. 1a and 1b show the calculated values $\sigma_{K^+p}^t = \sigma_{K^+p}^{el}$ (a) and $\sigma_{K^+n}^t = \sigma_{K^+n}^{el} + \sigma_{K^+n \rightarrow K^0p}$ (b). The cross sections $\sigma_{KN}^{I=0}$ in Fig. 1c were calculated through the relation $\sigma_{KN}^{I=0} = 2\sigma_{K^+n}^t - \sigma_{K^+p}^t$ in accordance with the data from Refs. [10, 11, 13].

The solid and dotted curves in Fig. 1 correspond to the results obtained with the use of parameters from Ref. [8]. The solid and dotted curves show the contributions of the

¹ With these amplitudes \hat{f} the differential cross section for binary reaction is $d\sigma/d\Omega = |\varphi_2^+ \hat{f} \varphi_1|^2 q_2/q_1$. Here: $\varphi_{1,2}$ are the spinors (and isospinors) of the initial and final nucleon and $\varphi_i^+ \varphi_i \equiv 1$; $q_{1,2}$ are the initial and final relative momenta. Throughout the paper we use the word "amplitude" for the matrix element $\varphi_2^+ \hat{f} \varphi_1$ and for the operator \hat{f} as well.

partial waves with $0 \leq l \leq 3$ and $0 \leq l \leq 1$, respectively. As one can see from Fig. 1 the d - and f -wave contributions are negligible at $p_{\text{LAB}} < 0.7$ GeV/ c . The dashed curves show the results obtained with the phase shifts from Ref. [5], where only s and p waves were included. Below, calculating the Kd cross sections, we use the KN parameters from Ref. [8].

TABLE: s -wave scattering lengths $a_I \equiv a_0^{(I)}$ and p -wave scattering volumes $v_I^\pm \equiv a_{1\pm}^{(I)}$ from Refs. [5, 8].

Ref.	a_1 (fm)	v_1^- (fm ³)	v_1^+ (fm ³)	a_0 (fm)	v_0^- (fm ³)	v_0^+ (fm ³)
[5]	-0.328	-0.02	0.015	-0.06	0.123	-0.010
[8]	-0.308	-0.092	0.103	-0.1048	0.183	-0.029

3 Amplitudes of the Kd reactions

3.1 The pole amplitudes of the break-up reactions

The pole diagrams for the $Kd \rightarrow KNN$ reactions are shown in Fig. 2a, where M_1 and M_2 also stand for the corresponding invariant amplitudes (the particle momenta are given in the deuteron rest frame). Hereafter we consider the deuteron and nucleons as nonrelativistic particles and kaons as relativistic ones. To calculate the Kd amplitudes, we use the deuteron wave function (DWF) $\Psi(\mathbf{q})$ in the form

$$\Psi(\mathbf{q}) = \frac{1}{\sqrt{2}} \varphi_2^+ \hat{\Psi}(\mathbf{q}) \varphi_1^c, \quad \hat{\Psi}(\mathbf{q}) = \frac{u(q)}{\sqrt{2}} (\boldsymbol{\epsilon} \boldsymbol{\sigma}) - \frac{w(q)}{2} \left[\frac{3(\mathbf{q} \boldsymbol{\epsilon})(\mathbf{q} \boldsymbol{\sigma})}{q^2} - (\boldsymbol{\epsilon} \boldsymbol{\sigma}) \right] \quad (6)$$

($q = |\mathbf{q}|$). Here: $\varphi_{1,2}$ are the nucleon spinor-isospinors ($\varphi_i^+ \varphi_i \equiv 1$); the notation φ^c means the charge-conjugated spinor-isospinor $\varphi^c \equiv \tau_2 \sigma_2 \varphi^*$; \mathbf{q} and $\boldsymbol{\epsilon}$ are the relative momentum of the nucleons and polarization vector of the deuteron, respectively; $u(q)$ and $w(q)$ are the s - and d -wave parts of the DWF, respectively, normalized as $\int d^3q [u^2(q) + w^2(q)] = (2\pi)^3$.

The invariant amplitudes M_1 and M_2 with DWF (6) read²

$$M_1 = 2\sqrt{m} \varphi_1^+ \hat{M}_{KN_1} \hat{\Psi}(\mathbf{p}_2) \varphi_2^c, \quad M_2 = -2\sqrt{m} \varphi_2^+ \hat{M}_{KN_2} \hat{\Psi}(\mathbf{p}_1) \varphi_1^c. \quad (7)$$

Here: m is the nucleon mass; φ_i is the spinor-isospinor of the i -th final nucleon; $\hat{M}_{KN_i} = 8\pi\sqrt{s_{KN_i}} \hat{f}_{KN_i}$ is the KN -scattering (on the i -th nucleon) invariant amplitude; $\sqrt{s_{KN_i}}$ is the invariant mass of the KN_i system. The cross sections, expressed through the invariant amplitudes, are given in Subsect. 1 of Appendix. The amplitude M_2 in Eqs. (7) can be obtained from M_1 by interchanging the nucleons, i.e. $M_2 = -M_1(N_1 \leftrightarrow N_2)$. Thus, the amplitude $M_1 + M_2$ is antisymmetric with respect to nucleons transposition in accordance with the Pauli principle. Further, calculating the interference of the amplitudes M_1 and

² When writing out the amplitudes of the reactions on the deuteron we follow the diagrammatic technique of Ref. [22].

M_2 , it is convenient to rewrite one of the them, say M_2 , with the help of identity $\varphi_2^+ \hat{A} \varphi_1^c \equiv \varphi_1^+ \hat{A}^c \varphi_2^c$, where \hat{A} is an arbitrary operator, containing the Pauli spin ($\boldsymbol{\sigma}$) and isospin ($\boldsymbol{\tau}$) matrices, and $A^c \equiv \sigma_2 \tau_2 A^T \sigma_2 \tau_2$ (note that $I^c = I$, $\boldsymbol{\sigma}^c = -\boldsymbol{\sigma}$ and $\boldsymbol{\tau}^c = -\boldsymbol{\tau}$). Then we can rewrite the amplitudes (7) as

$$M_1 = c_1 \varphi_1^+ \hat{f}_{KN_1} \hat{\Psi}(\mathbf{p}_2) \varphi_2^c, \quad M_2 = -c_2 \varphi_1^+ \hat{\Psi}^c(\mathbf{p}_1) \hat{f}_{KN_2}^c \varphi_2^c, \quad (8)$$

where $c_i = 16\pi \sqrt{m s_{KN_i}}$. The expressions for the particle momenta used to calculate the amplitudes are given in Subsect. 2 of Appendix. The squares and interferences of the amplitudes for the reactions $Kd \rightarrow KNN$ with unpolarized particles are given in Subsect. 3 of Appendix ³.

Strictly speaking, in the case of the reaction $K^+d \rightarrow K^+pn$, the pole amplitudes $M_{1,2}$ (8) should also contain the term proportional to the Coulomb K^+p -scattering amplitude f_C . It can be included by the replacement $\hat{f}_{KN_i} \rightarrow \hat{f}_{KN_i} + \frac{1}{2} f_C (1 + \tau_3)$ in the hadronic K^+N -scattering amplitudes. Since $f_C \sim 1/t$, where $t = (k - k_1)^2$ is the square of the four-momentum transfer, the Coulomb effects may be essential at small scattering angles of the outgoing kaons (small t). Thus, the measured cross sections of the reaction $K^+d \rightarrow K^+pn$ should depend on the experimental conditions.

Note that in the break-up reaction $Kd \rightarrow KNN$ we always have $t \leq -|t|_{min} < 0$, since $\sqrt{s_{NN}} \neq m_d$ (m_d , $\sqrt{s_{NN}}$ are the deuteron mass and the effective mass of the NN system). Thus, the total Coulomb cross section $\sigma_C(K^+d \rightarrow K^+pn)$ is finite unlike the case of the elastic scattering processes for which it diverges at zero scattering angles (at $t \rightarrow 0$). An estimate of the Coulomb cross section $\sigma_C(K^+d \rightarrow K^+pn)$ is given in Subsect. 6 of Appendix. In the following we neglect the Coulomb effects when calculating the Kd cross sections.

3.2 The final-state interaction (FSI) of nucleons

At low energies the important effect should come from the nucleon-nucleon final state interaction (FSI) due to large NN -scattering lengths. The famous FSI effect is responsible for the near-threshold enhancement in the mass spectra $d\sigma/d\sqrt{s_{NN}}$ (Migdal-Watson effect [24, 25]) of the meson production reactions $NN \rightarrow NNx$ and increases the reaction cross section in the near-threshold region. The role of secondary rescatterings was also investigated in reactions on the deuteron (for example, in the reaction $\pi^-d \rightarrow \pi^-pn$ [26]). In this paper we take into account only the NN -rescattering amplitudes and neglect the KN -rescatterings, since the KN -scattering lengths are relatively small, $a_{KN} \ll a_{NN}$.

The NN FSI diagram is shown on Fig. 2b (the diagram M_R). We consider only the s -wave NN rescattering. It is convenient to write the invariant amplitude of the s -wave scattering $N_3 N_4 \rightarrow N_1 N_2$ in the form

$$M_{NN}^{(S)} = 8\pi \sqrt{s_{NN}} \left[f_{NN}^{(0)}(p) (\varphi_4^{c+} \frac{\boldsymbol{\sigma}}{\sqrt{2}} \varphi_3) (\varphi_1^+ \frac{\boldsymbol{\sigma}}{\sqrt{2}} \varphi_2^c) + f_{NN}^{(1)}(p) (\varphi_4^{c+} \frac{\boldsymbol{\tau}}{\sqrt{2}} \varphi_3) (\varphi_1^+ \frac{\boldsymbol{\tau}}{\sqrt{2}} \varphi_2^c) \right], \quad (9)$$

³ There are relations, derived in Ref. [23], for the differential cross sections of reactions $Kd \rightarrow KNN$ in the impulse approximation with spin and isospin variables taken into account. However, they can not be applied when d -wave part of WFD or the rescatterings are included.

where \sqrt{s}_{NN} is the invariant mass of the NN system (we take $\sqrt{s}_{NN} = 2m$ for the non-relativistic nucleons) and $f_{NN}^{(I=0,1)}(p)$ are the NN -scattering amplitudes with isospin I and relative momentum p , normalized as $d\sigma/d\Omega = |f|^2$. The first (second) term in Eq. (9) corresponds to the NN -scattering amplitude with isospin $I = 0(1)$ and total spin $S_{NN} = 1(0)$ in accordance with the Pauli principle.

Let the $N_3 N_4 \rightarrow N_1 N_2$ amplitude be given in the general form $M_{NN} = (\varphi_4^c \hat{B}_2 \varphi_3) (\varphi_1^+ \hat{B}_1 \varphi_2^c)$, where the operators $\hat{B}_{1,2}$ contain the nucleon spin (σ) and isospin (τ) Pauli matrices. Then, making use of the notations $\hat{\Psi}(\mathbf{p}_i)$ and \hat{M}_{KN} from Eqs. (6) and (7), one can obtain the NN FSI amplitude M_R in the form

$$M_R = \frac{-1}{\sqrt{m}} \int \frac{d^3 \mathbf{p}_4}{(2\pi)^3} \frac{\text{Tr}\{\hat{\Psi}(\mathbf{p}_4) \hat{B}_2 \hat{M}_{KN}\}}{2m\varepsilon_3 - \mathbf{p}_3^2 + i0} (\varphi_1^+ \hat{B}_1 \varphi_2^c). \quad (10)$$

Here: \mathbf{p}_i and ε_i ($i = 1, 2, 3, 4$) are the nucleon momenta in the deuteron rest frame (see Fig. 2b) and kinetic energies, respectively; the nucleon with the momentum \mathbf{p}_4 is "on-shell"; $\varepsilon_3 = \varepsilon_1 + \varepsilon_2 - \varepsilon_4$, $\varepsilon_{1,2,4} = p_{1,2,4}^2/2m$; $\text{Tr}\{(\dots)\} \equiv \text{Tr}\{\hat{T}\} \text{Tr}\{\hat{S}\}$, where $\text{Tr}\{\hat{T}\}$ ($\text{Tr}\{\hat{S}\}$) is a trace of isospin (spin) part \hat{T} (\hat{S}) of the matrix expression $(\dots) = \hat{T}\hat{S}$. Taking the NN amplitude, given by Eq. (9), we should make the replacement

$$\begin{aligned} \text{Tr}\{\hat{\Psi} \hat{B}_2 \hat{M}_{KN}\} (\varphi_1^+ \hat{B}_1 \varphi_2^c) &\rightarrow 8\pi m \left[f_{NN}^{(0)off}(q, p) \text{Tr}\{\hat{\Psi} \boldsymbol{\sigma} \hat{M}_{KN}\} (\varphi_1^+ \boldsymbol{\sigma} \varphi_2^c) \right. \\ &\quad \left. + f_{NN}^{(1)off}(q, p) \text{Tr}\{\hat{\Psi} \boldsymbol{\tau} \hat{M}_{KN}\} (\varphi_1^+ \boldsymbol{\tau} \varphi_2^c) \right] \end{aligned} \quad (11)$$

in Eq. (10). Here $f_{NN}^{(I)off}(q, p)$ is the "off-shell" NN amplitude with isospin I and $q(p)$ is the relative momentum of the intermediate (final) nucleons in the diagram M_R . To simplify the calculations, we take into account only the s -wave KN scattering in the amplitude M_R . We shall comment this approximation below in Sect. 4. In this case the operator \hat{M}_{KN} contains no spin matrices $\boldsymbol{\sigma}$ and $\text{Tr}\{\hat{\Psi} \boldsymbol{\tau} \hat{M}_{KN}\} = 0$, since the spin trace $\text{Tr}\{\hat{\Psi}\} \sim \text{Tr}\{\boldsymbol{\sigma}\} = 0$. It means that the term, proportional to $f_{NN}^{(1)}$, vanishes in the amplitude M_R . Thus, in our approximation the NN FSI takes place only in the triplet $NN(^3S_1)$ state with isospin $I = 0$ in the reaction $K^+ d \rightarrow K^+ p n$ and is absent in the reaction $K^+ d \rightarrow K^0 p p$. For the first term of the right-hand part of Eq. (11) we get

$$\text{Tr}\{\hat{\Psi} \boldsymbol{\sigma} \hat{M}_{KN}\} (\varphi_1^+ \boldsymbol{\sigma} \varphi_2^c) = 8\pi \sqrt{s}_{KN} \left[3f_0^{(1)} + f_0^{(0)} \right] (\varphi_1^+ \hat{\Psi} \varphi_2^c) \quad (12)$$

(here an additional factor 2 comes from isospin trace $\text{Tr}\{I\} = 2$), where $f_0^{(I)}$ are the s -wave KN amplitudes with isospins $I = 0, 1$ (see Eqs. (3)).

The "off-shell" NN amplitude $f_{NN}^{(0)off}(q, p)$ is chosen here in the form, corresponding to the scattering on the separable Yamaguchi potential. For the "on-shell" amplitude $f_{NN}^{(0)}(p)$ we use the known parameters [27]. Then

$$f_{NN}^{(0)off}(q, p) = \frac{p^2 + \beta^2}{q^2 + \beta^2} f_{NN}^{(0)}(p), \quad f_{NN}^{(0)}(p) = \frac{1}{1/a_{NN}^{(0)} + \frac{1}{2}r_0 p^2 - ip}, \quad (13)$$

$$\beta \approx 240 \text{ MeV}, \quad a_{NN}^{(0)} = -5.4 \text{ fm}, \quad r_0 = 1.7 \text{ fm}.$$

Finally, applying Eqs. (10), (11), (12) and (13), we obtain the amplitude M_R in the form

$$M_R = c A_R \varphi_1^+ \left[\hat{L}(-p^2) - \hat{L}(\beta^2) \right] \varphi_2^c, \quad A_R = \frac{1}{4} f_{NN}^{(0)}(p) \left[3f_0^{(1)} + f_0^{(0)} \right],$$

$$\hat{L}(x) = 8\pi \int \frac{d^3 \mathbf{q}}{(2\pi)^3} \frac{\hat{\Psi}(\mathbf{q} + \Delta)}{(q^2 + x - i0)}, \quad \Delta = \frac{\mathbf{p}_1 + \mathbf{p}_2}{2}, \quad \mathbf{p} = \frac{\mathbf{p}_1 - \mathbf{p}_2}{2}, \quad (14)$$

where $c = 16\pi\sqrt{m} s_{KN}$. Here we evaluate the KN amplitudes $f_0^{(I)}$ for the target nucleon at rest in the deuteron rest frame. The integral $\hat{L}(x)$ is calculated in Subsect. 4 of Appendix, where the analytical expression is given in the case of the Bonn [28] or Paris [29, 30] DWF.

3.3 Elastic (coherent) K^+d scattering

Close to threshold contribution of the elastic process $K^+d \rightarrow K^+d$ dominates in the total cross section σ_{Kd}^t . We shall use a single-scattering approximation for the elastic scattering amplitude M_{K+d}^{el} (see the diagram in Fig. 3), neglecting relatively small contributions of kaon rescattering and meson exchange currents [31] to the integrated cross section σ_{K+d}^{el} . In our notations the amplitude M_{K+d}^{el} reads

$$M_{K+d}^{el} = 2 \int \frac{d^3 \mathbf{p}}{(2\pi)^3} \text{Tr} \{ \hat{\Psi}_2^+(\mathbf{q}_2) \hat{M}_{KN} \hat{\Psi}_1(\mathbf{q}_1) \} \quad (\mathbf{q}_1 = \mathbf{p} - \frac{\mathbf{P}}{2}, \quad \mathbf{q}_2 = \mathbf{p} - \frac{\mathbf{P}_1}{2}), \quad (15)$$

where $\hat{\Psi}^{1,2}(\mathbf{q}_{1,2})$ are the operators in the DWF (6) of the initial and final deuteron, respectively; $\hat{M}_{K+N} = 8\pi\sqrt{s_{KN}} \hat{f}_{K+N}$ is the KN -scattering operator (the particle momenta are denoted in Fig. 3).

The expression for the $K^+d \rightarrow K^+d$ differential cross section $d\sigma/d\Omega$ can be found, for example, in Refs. [23, 32] for the s -wave DWF, and in Ref. [33] for the case with the d -wave part of DWF included. For the unpolarized particles this cross section is $d\sigma/d\Omega = |M_{K+d}^{el}|^2 / (8\pi\sqrt{s_{Kd}})^2$, where Ω is the CM solid angle, and can be written as

$$\frac{d\sigma}{d\Omega} = \frac{4s_{KN}}{s_{Kd}} \left[|A_p + A_n|^2 \left[\Phi_S^2(q) + \Phi_Q^2(q) \right] + \frac{2}{3} |B_p + B_n|^2 \Phi_M^2(q) \right]. \quad (16)$$

Here: $\mathbf{q} = \frac{1}{2}(\mathbf{k} - \mathbf{k}_1)$; $\sqrt{s_{Kd}}$ is the total CM energy; $A_{p,n}$ and $B_{p,n}$ are the coefficients in the K^+N amplitudes $\hat{f}_{p,n} = A_{p,n} + B_{p,n}(\mathbf{n}\sigma)$ (we calculate them at fixed momentum $\mathbf{p} = \frac{1}{2}(\mathbf{P}_1 + \mathbf{P}_2)$ of the intermediate nucleon Fig. 3). The form factors $\Phi_S(q)$, $\Phi_Q(q)$ and $\Phi_M(q)$ in Eq. (16) are

$$\Phi_S = F_a + F_b, \quad \Phi_Q = 2F_c - \frac{F_d}{\sqrt{2}}, \quad \Phi_M = F_a - \frac{F_b}{2} + \frac{F_c}{\sqrt{2}} + \frac{F_d}{2}, \quad (17)$$

where

$$F_a = 4\pi \int dr j_0(qr) u^2(r), \quad F_b = 4\pi \int dr j_0(qr) w^2(r),$$

$$F_c = 4\pi \int dr j_2(qr) u(r) w(r), \quad F_d = 4\pi \int dr j_2(qr) w^2(r). \quad (18)$$

Here: $u(r)$ and $w(r)$ are the s - and d -wave components of the DWF in coordinate representation, normalized as $4\pi\int dr [u^2(r) + w^2(r)] = 1$; j_0 and j_2 are the zeroth and second order spherical Bessel functions, respectively. In the case of the Bonn [28] or Paris [29, 30] DWF the analytical expressions for the integrals (18) are given in Subsect. 5 of Appendix.

4 Cross sections of the Kd reactions

4.1 The results of calculations and comparison with the data

Here we present the results of our calculations of the K^+d cross sections, based on the formulas from Sects. 2 and 3. We use the KN phase shifts from Ref. [8] and take into account only s - and p -wave KN amplitudes, while d - and f -wave contributions are negligibly small at the energies of interest and are neglected. We also use the DWF of the Bonn potential [28] (full model) with s - and d -wave components included.

Fig. 4 shows the total cross sections of the reactions $K^+d \rightarrow K^+pn$ (a) and $K^+d \rightarrow K^0pp$ (b). The symbols corresponds to the experimental data from Refs. [21] (Fig. 4a) and [21, 34, 35, 36] (Fig. 4b). The curves show the results of calculations. In Fig. 4a the curves show the contributions of the amplitudes $M_1 + M_2$ (dashed), M_R (dotted), $M_1 + M_2 + M_R$ (solid), $M_1 + M_2 + M_R$ with the s -wave DWF (dashed-dotted), $M_1 + M_2 + M_R$ with the s -wave KN amplitudes (dashed curve "S"). In Fig. 4b the curves show the contributions of the amplitude $M_1 + M_2$. Here are also given the results, obtained with s -wave DWF (dashed-dotted curve) and with the s -wave KN amplitude (dashed curve "S"). Comparing the solid and dashed-dotted curves in Fig. 4, one finds that the influence of the deuteron d wave on the results is very small.

Fig. 4a shows that the contribution of the NN FSI amplitude M_R essentially affects the calculated cross section. The term M_R destructively interferes with the pole amplitudes $M_{1,2}$ and decreases the cross section at $p_{\text{LAB}} < 200$ MeV/ c by several times. Remember that the diagram M_R , in which we take into account only the s -wave KN scattering, contains the NN rescattering only in the triplet 3S_1 state ($S_{NN} = 1, I = 0$). However, the NN -scattering length in the singlet 1S_0 -state ($S_{NN} = 0, I = 1$) $a_{NN}^{(1)} = 24$ fm [27] and is large in comparison with the triplet value $a_{NN}^{(0)}$ (see Eqs. (13)). Thus, one needs the arguments to neglect the $NN(^1S_0)$ rescattering.

This approximation should be reasonable in the momentum range where the p -wave KN amplitude is small. Comparing the solid curve and the dashed one, marked by "S", in Fig. 4a, we find the influence of the p -wave KN -scattering in the reaction $K^+d \rightarrow K^+pn$ to be small at $p_{\text{LAB}} < 250$ MeV/ c . From this indirect estimation we expect that the $NN(^1S_0)$ -rescattering correction is not essential in this range, but this approximation is less reliable at larger momenta p_{LAB} . In more accurate calculation of the NN FSI correction the p -wave KN amplitude and $NN(^1S_0)$ interaction should be also included. We postpone this to a future study.

Figs. 5a and 5b show the total ($\sigma_{K^+d}^{\text{tot}}$) and the elastic ($\sigma_{K^+d}^{\text{el}}$) K^+d cross sections, respectively. The symbols are the experimental data from Refs. [10, 11, 12, 21, 34] (Fig. 5a)

and [21, 37] (Fig. 5b). Here, the calculated cross section $\sigma_{K^+d}^{tot}$ is taken as a sum of the $K^+d \rightarrow K^+pn$, $K^+d \rightarrow K^0pp$ and $K^+d \rightarrow K^+d$ cross sections, shown by the solid curves in Figs. 4a, 4b and 5b. The dashed-dotted curves in Fig. 5 are the results, obtained with the s -wave DWF. The dashed curve in Fig. 5a shows the result for $\sigma_{K^+d}^{tot}$ in which the contribution of the $K^+d \rightarrow K^+pn$ cross section is not corrected for NN FSI.

Let us comment here the results of Ref. [5], where data on the total cross section $\sigma_{K^+d}^{tot}$ were analysed and $\sigma_{K^+d}^{tot}$ was evaluated through the unitarity with single- and double-scattering $K^+d \rightarrow K^+d$ amplitudes employed. The unitarity cuts of the single- and double-scattering terms correspond to the contributions (summed over the K^+pn and K^0pp channels) of the squares $|M_1|^2 + |M_2|^2$ and of the interference term $2\text{Re}(M_1^* M_2)$, where $M_{1,2}$ are the pole amplitudes. Our comment is the following.

1. The cross section $\sigma_{K^+d}^{tot}$, calculated in Ref. [5], does not include the contribution of the elastic K^+d scattering, which dominates at low momenta $p_{\text{LAB}} < 100$ MeV/ c . Results of our computations at $p_{\text{LAB}} = 100$ MeV/ c are shown in Figs. 4 and 5. They give $\sigma_{K^+d}^{el} = 34.4$ mb, $\sigma_{K^+d}^{inel} = \sigma(K^+pn + K^0pp) = 0.9$ mb (9.7 mb) and $\sigma_{K^+d}^{tot} = 35.3$ mb (44.1 mb) with (without) NN FSI diagram M_R included. On the other hand, in Ref. [5] (see Fig. 5 there) one finds $\sigma_{K^+d}^{tot} = \sigma_{K^+d}^{inel} \approx 27$ mb. This value of $\sigma_{K^+d}^{inel}$ is too large due to the following reasons. Firstly, the elementary KN amplitude, used in Ref. [5], corresponds to the real (not virtual) target nucleon (see Eq. (17) there). Secondly, they average the K^+N cross section over the Fermi momentum distribution (see Eq. (19) there) in the range $0 < p < \infty$, neglecting the kinematical boundaries. Thus, the cross section in Ref. [5] is overestimated in the nearthreshold region, where the kinematical boundaries are important.

2. The double-scattering K^+d amplitude is considered in Ref. [5] under the following assumptions. The propagator of the intermediate kaon is taken in a "static nucleon" approximation. Thus, the contribution of this diagram to $\sigma_{K^+d}^{tot}$ depends on the energy like 2-particle phase space instead of 3-particle (KNN) one as it should be. The elementary K^+N amplitudes modified by the $K^+N(I=0)$ -resonance contribution are taken out of the integral over the momenta in the intermediate KNN state and taken at fixed nucleon momenta. This approximation is widely used for the hadronic amplitudes, usually being smooth functions in comparison with the rapid p dependence of the nuclear wave functions. However, in the case of a narrow ($\Gamma \sim 1$ MeV) K^+N resonance this approximation can be not reliable.

Summarising the results of this Sect., we conclude that the approach, based on the pole diagrams and modified by the NN FSI term (simplified as discussed above), gives a reasonable description of the existing data on the integrated K^+d cross sections in the range $p_{\text{LAB}} < 800$ MeV/ c . The NN FSI effect is found to be large. It would be useful to have the data on the $\sigma_{K^+d}^{tot}$ and $K^+d \rightarrow K^+pn$ cross section in the range, say $p_{\text{LAB}} < 400$ MeV/ c (where they are absent now), for more detailed study of the NN FSI effect and comparison with the data.

4.2 On the extraction of the isoscalar $KN(I=0)$ scattering length

To determine the isoscalar KN scattering length a_0 one needs the additional data on the kaon-neutron scattering, but the neutron targets do not exist. Thus, to extract the value of a_0 , one should compare the theoretical predictions with the data on the cross sections for the existing targets and the deuteron one is preferable. As a source of slow kaons the decay $\phi(1020) \rightarrow K^+K^-$ at rest can be used and the $\phi(1020)$ mesons can be produced in the e^+e^- -collisions at DAΦNE accelerator in Frascati.

Fig. 6 show our predictions for the K^+d cross sections at the initial momentum $p_{\text{LAB}} = 127 \text{ MeV}/c$, which is the kaon momentum in the $\phi(1020)$ decay. At this momentum the p -wave KN amplitudes are negligibly small and we use here only the s -wave amplitudes. Figs. 6a and 6b show the $K^+d \rightarrow K^+pn$ (a) and $K^+d \rightarrow K^0pp$ (b) cross sections. The total and the elastic K^+d cross sections are given in Figs. 6c and 6d, respectively. The results are presented as functions of a_0 in some range around the "realistic" values, given in the Table. The results are given for two fixed values $a_1 = -0.328 \text{ fm}$ (curves 1) and $a_1 = -0.308 \text{ fm}$ (curves 2), taken from the Table. The solid and dashed curves in Figs. 6a and 6c show the results obtained with and without NN FSI, taken into account. Thus, the NN FSI amplitude strongly affects the $K^+d \rightarrow K^+pn$ and total K^+d cross sections for slow kaons.

5 Conclusion

The theoretical predictions for the K^+d cross sections were presented in the "quasi-elastic" energy range $p_{\text{LAB}} < 0.8 \text{ GeV}/c$, where the particle-production processes in the elementary KN interactions can be neglected. We used the approach, which employs the pole $Kd \rightarrow KNN$ amplitudes, the NN FSI correction, and the "realistic" KN phase shifts. In our approximation we neglected the p -wave KN scattering, when calculating the NN FSI correction. Since the s -wave KN -scattering amplitude is non-spin-flip the NN FSI takes place only in the $NN(^3S_1)$ state, forbidden for the reaction $K^+d \rightarrow K^0pp$ due to the Pauli principle. This approximation should be reasonable in the low-momentum range (estimated in Sect. 4), where the KN -scattering amplitude is predominantly s -wave.

A reasonable description of the data on the integrated $K^+d \rightarrow K^+pn$ and $K^+d \rightarrow K^0pp$ cross sections as well as on the total and elastic K^+d cross sections were obtained. The NN FSI diagram affects strongly the value of the $K^+d \rightarrow K^+pn$ cross section in the low energy region and interferes destructively with the pole diagrams. However, data on the $K^+d \rightarrow K^+pn$ cross section are available only at higher energies $p_{\text{LAB}} > 600 \text{ MeV}/c$, where our calculations of NN FSI are less reliable and some defects of the theoretical description are seen. It would be interesting to measure the $K^+d \rightarrow K^+pn$ cross section at low energies, say $p_{\text{LAB}} < 400 \text{ MeV}/c$, where the NN FSI effect is large, to investigate the role of this mechanism.

Predictions were also given for the integrated cross sections of the K^+d reactions with slow kaons as functions of the isoscalar KN -scattering length a_0 . These results would be usefull for extraction of the a_0 value from the data. The corresponding experiments

with slow kaon beam from the $\phi(1020)$ decays may be proposed, say, for the DAΦNE accelerator. At this energy ($p_{\text{LAB}} = 127 \text{ MeV}/c$) the NN FSI effect is very strong in the reaction $K^+d \rightarrow K^+pn$ as it is seen from Fig. 4a. Thus, study of this reaction at the DAΦNE machine would be very important.

In the more detailed treatment of NN FSI the p -wave KN scattering and $NN(^1S_0)$ interaction should be also taken into account. We postpone this for a future study. However, these improvements should not affect essentially our results for the K^+d cross sections at the energy of kaons from $\phi(1020)$ decay and the conclusion about the large magnitude of the NN FSI effect.

Authors acknowledge support of the Federal Agency of Atomic Energy of Russian Federation. Participations of V.E.T. and A.E.K. were supported by DFG-RFBR grant no. 05-02-04012 (436 RUS 113/820/0-1(R)).

Appendix

1. Cross sections and phase spaces.

Calculating the Kd cross sections, we use the invariant amplitudes with Feynman normalization. The cross section σ_n of the process $a+b \rightarrow 1 + \dots + n$ reads

$$\sigma_n = \frac{1}{4q_{ab}\sqrt{s}} \int |M|^2 d\tau_n, \quad d\tau_n = I_n (2\pi)^4 \delta^{(4)}(P_i - P_f) \prod_{i=1}^n \frac{d^3\mathbf{p}_i}{(2\pi)^3 2E_i}. \quad (\text{A.1})$$

Here M is the invariant amplitude; \sqrt{s} is the total CM energy; q_{ab} is the initial relative momentum and $q_{ab} = \lambda(s, m_a^2, m_b^2)$, where $\lambda(z, x, y) = \sqrt{(z-x-y)^2 - 4xy} / 2\sqrt{z}$ and $m_a(m_b)$ is the mass of the particle $a(b)$; $d\tau_n$ is the element of the final n -particle phase space; $P_i(P_f)$ is the total initial (final) four-momentum; E_i and \mathbf{p}_i are the total energy and momentum of the i -th final particle; the factor $I_n \equiv 1/n_1! \dots n_k!$ takes into account the identity of final particles, where n_i is the number of particles of the i -th type ($n_1 + \dots + n_k = n$). Then, the cross section σ of the reaction $Kd \rightarrow KNN$ with unpolarized particles can be written as

$$\sigma = \int \frac{d\sigma}{d\sqrt{s}_{NN}} d\sqrt{s}_{NN}, \quad \frac{d\sigma}{d\sqrt{s}_{NN}} = \frac{I_n}{2(4\pi)^4 Q s} \int |\overline{M}|^2 Q_1 p dz_1 dz d\varphi, \quad (\text{A.2})$$

where $z = \cos \theta$, $z_1 = \cos \theta_1$. Here: $|\overline{M}|^2$ is the square of the reaction amplitude M with unpolarized particles; $Q = |\mathbf{Q}|$ and $Q_1 = |\mathbf{Q}_1|$, where \mathbf{Q} and \mathbf{Q}_1 are the CM momenta of the incoming and outgoing kaon, respectively; θ_1 is the CM polar angle of the outgoing kaon; $p = |\mathbf{p}|$; \mathbf{p} , θ and φ are the momentum and the angles (polar and azimuthal) of the outgoing nucleon, say N_1 , in the NN rest frame.

2. Kinematics.

Let us express all the momenta used to calculate the $Kd \rightarrow KNN$ amplitude, through the variables \sqrt{s}_{NN} , z_1 , z and φ of the integrals (A.2). One can write

$$Q = \lambda(s, m_K^2, m_d^2), \quad Q_1 = \lambda(s, m_K^2, s_{NN}), \quad p = \sqrt{m(\sqrt{s}_{NN} - 2m)}, \quad (\text{A.3})$$

where m_K (m_d) is the kaon (deuteron) mass and the function $\lambda(\dots)$ is defined after Eq. (A.1). Let us introduce the notations: $\mathbf{p}'_{1,2}$ and $\mathbf{p}_{1,2}$ – the momenta of the final nucleons in the reaction and in the deuteron rest frames, respectively; $\mathbf{q}'_{1,2}$ and $\mathbf{q}_{1,2}$ – the initial and final nucleon momenta, respectively, in the rest frame of the $KN_{1,2} \rightarrow KN_{1,2}$ subprocess in the diagram $M_{1,2}$ (Fig. 2). Then we write:

$$\mathbf{p}'_{1,2} = \pm \mathbf{p} - \frac{\mathbf{Q}_1}{2}, \quad \mathbf{p}_{1,2} = \mathbf{p}'_{1,2} + \frac{\mathbf{Q}}{2}, \quad \mathbf{q}_{1,2} = \frac{\omega \mathbf{p}'_{1,2} - m \mathbf{Q}_1}{m + \omega}, \quad \mathbf{q}'_{1,2} = \mathbf{q}_{1,2} + \mathbf{Q}_1 - \mathbf{Q}, \quad (\text{A.4})$$

where $\omega = \sqrt{m_K^2 + p_{\text{LAB}}^2}$ is the kaon total energy. The values $q_i = |\mathbf{q}_i|$, $z_{KN_i} = (\mathbf{q}'_i \mathbf{q}_i) / q'_i q_i$ and $\mathbf{n}_i = [\mathbf{q}'_i \times \mathbf{q}_i] / |[\mathbf{q}'_i \times \mathbf{q}_i]|$ are used to calculate the $K^+ N_i$ -scattering amplitude ($i = 1, 2$), according to Eqs. (3).

3. The square of the $Kd \rightarrow KNN$ amplitude

Here we write out the square $|\overline{M}|^2$ of the amplitude $M = M_1 + M_2 + M_R$ for unpolarized particles, applying the formulas from Sects. 2 and 3. Hereafter, we exclude the isospin variables and fix the nucleons with momenta \mathbf{p}_1 and \mathbf{p}_2 in the reaction $K^+ d \rightarrow K^+ pn$ as proton and neutron, respectively. Then, $I_n = 1(\frac{1}{2})$ in Eq. (A.2) for the reaction $K^+ d \rightarrow K^+ pn$ ($K^+ d \rightarrow K^0 pp$). Let $A_{(i)}$ and $B_{(i)}$ be the coefficients in the $K^+ N_i$ amplitude $\hat{f}_{KN_i} = A_{(i)} + B_{(i)}(\mathbf{n}_i \boldsymbol{\sigma})$. Then: $A_{(1)} = A_1$ and $B_{(1)} = B_1$ ($A_{(2)} = \frac{1}{2}(A_1 + A_0)$ and $B_{(2)} = \frac{1}{2}(B_1 + B_0)$) for the $K^+ p$ ($K^+ n$)-scattering subprocess in the diagram M_1 (M_2) for the reaction $K^+ d \rightarrow K^+ pn$; $A_{(i)} = \frac{1}{2}(A_1 - A_0)$ and $B_{(i)} = \frac{1}{2}(B_1 - B_0)$ for the charge exchange subprocess $K^+ n \rightarrow K^0 p$ in the reaction $K^+ d \rightarrow K^0 pp$; the values A_I and B_I are given in Eqs. (3). For the different terms of the expression $|\overline{M}|^2$ we obtain (hereafter $\text{Tr}\{(\dots)\}$ means the trace of the 2×2 matrix (\dots) with spin indices)

$$\begin{aligned} |\overline{M_i}|^2 &= c^2 \text{Tr}\{\hat{\Psi}(\mathbf{p}_j) \hat{\Psi}^+(\mathbf{p}_j) \hat{f}_{KN_i}^+ \hat{f}_{KN_i}\} \quad (i \neq j = 1, 2), \\ \overline{M_1 M_2^+} &= \pm c^2 \text{Tr}\{\hat{\Psi}(\mathbf{p}_2) (A_{(2)} - B_{(2)} \hat{n}_2)^+ \hat{\Psi}^+(\mathbf{p}_1) (A_{(1)} + B_{(1)} \hat{n}_1)\}, \\ \overline{M_i^+ M_R} &= c^2 A_R \text{Tr}\{\hat{\Psi}^+(\mathbf{p}_j) \hat{f}_{KN_i}^+ \hat{L}\} \quad (i \neq j = 1, 2), \\ |\overline{M_R}|^2 &= c^2 |A_R|^2 \text{Tr}\{\hat{L} \hat{L}^+\}, \quad \hat{L} = \hat{L}(-p^2) - \hat{L}(\beta^2), \end{aligned} \quad (\text{A.5})$$

where $\hat{n}_i = (\mathbf{n}_i \boldsymbol{\sigma})$. Here: the sign "–" in the expression for $\overline{M_1 M_2^+}$ corresponds to the case of the reaction $K^+ d \rightarrow K^0 pp$; the terms $\overline{M_i^+ M_R}$ and $|\overline{M_R}|^2$ are given for the reaction $K^+ d \rightarrow K^+ pn$; the quantities A_R and $\hat{L}(x)$ are given by Eqs. (14); calculating the factors c_i and c , defined in Eqs. (8) and (14), we use the value of s_{KN} for the nucleon at rest, i.e. $c_i = c = 16\pi\sqrt{m} s_{KN}$ and $s_{KN} = m_K^2 + m^2 + 2\omega m$.

Let us introduce the functions $f(p)$ and $g(p)$, rewriting $\hat{\Psi}(p)$ (6) in the form

$$\begin{aligned} \hat{\Psi}(\mathbf{p}) &= f(p)(\boldsymbol{\epsilon} \boldsymbol{\sigma}) + g(p) \frac{(\mathbf{p} \boldsymbol{\epsilon})(\boldsymbol{\epsilon} \boldsymbol{\sigma})}{p^2}, \\ f(p) &= \frac{u(p)}{\sqrt{2}} + \frac{w(p)}{2}, \quad g(p) = -\frac{3w(p)}{2}. \end{aligned} \quad (\text{A.6})$$

Finally, from Eqs. (A.5) and (A.6), we obtain

$$\begin{aligned}
\overline{|M_i|^2} &= c^2 [u^2(p_j) + w^2(p_j)] [|A_{(i)}|^2 + |B_{(i)}|^2] \quad (i \neq j=1, 2), \\
\text{Re}(\overline{M_1 M_2^+}) &= \pm c^2 \left[\text{Re}(A_{(1)} A_{(2)}^*) \left(u(p_2)u(p_1) + w(p_2)w(p_1) \frac{3z_p^2 - 1}{2} \right) \right. \\
&\quad + \frac{2g_1 g_2 z_p}{3p_1 p_2} \left((\mathbf{p}_2 [\mathbf{n}_2 \times \mathbf{p}_1]) \text{Im}(A_{(1)} B_{(2)}^*) - (\mathbf{p}_1 [\mathbf{n}_1 \times \mathbf{p}_2]) \text{Im}(B_{(1)} A_{(2)}^*) \right) \\
&\quad + \text{Re}(B_{(1)} B_{(2)}^*) \left[\frac{2}{3} (\mathbf{n}_1 \mathbf{n}_2) (f_1 f_2 + g_1 f_2 + f_1 g_2 + g_1 g_2 z_p^2) \right. \\
&\quad \left. \left. + \frac{4(\mathbf{p}_1 \mathbf{n}_1)(\mathbf{p}_2 \mathbf{n}_2)}{3} \left(\frac{g_1 f_2}{p_1^2} + \frac{f_1 g_2}{p_2^2} - \frac{g_1 g_2 z_p}{p_1 p_2} \right) \right] \right] \quad \left(z_p = \frac{(\mathbf{p}_1 \mathbf{p}_2)}{p_1 p_2} \right),
\end{aligned} \tag{A.7}$$

$$\begin{aligned}
\text{Re}(\overline{M_i^+ M_R}) &= c^2 \left[2 \text{Re} \left(A_R A_{(i)}^* \left[\left(f_j + \frac{g_j}{3} \right) A + \frac{g_j}{3} B \left(\frac{3(\mathbf{p}_j \boldsymbol{\Delta})^2}{p_j^2 \Delta^2} - 1 \right) \right] \right) \right. \\
&\quad \left. + \text{Im}(A_R B_{(i)}^* B) g_j \frac{(\mathbf{p}_j \boldsymbol{\Delta})}{p_j^2 \Delta^2} (\mathbf{p}_i [\mathbf{n}_i \times \mathbf{p}_j]) \right] \quad (i \neq j=1, 2),
\end{aligned}$$

$$\overline{|M_R|^2} = 2c^2 |A_R|^2 (|A|^2 + 2|B|^2),$$

where $f_{1,2} = f(p_{1,2})$, $g_{1,2} = g(p_{1,2})$. Here A and B are the coefficients in the expression for $\hat{L}(x)$, given below in Subsect. 4. If one neglects the d -wave part of DWF, Eqs. (A.7) give

$$\begin{aligned}
\overline{|M_i|^2} &= c^2 u^2(p_j) [|A_{(i)}|^2 + |B_{(i)}|^2] \quad (i \neq j=1, 2), \\
\overline{M_1 M_2^+} &= \pm c^2 u(p_1)u(p_2) \left[A_{(1)} A_{(2)}^* + \frac{1}{3} B_{(1)} B_{(2)}^* (\mathbf{n}_1 \mathbf{n}_2) \right], \\
\overline{M_i^+ M_R} &= c^2 A_R A_{(i)}^* A u(p_j), \quad \overline{|M_R|^2} = 2c^2 |A_R|^2 |A|^2.
\end{aligned} \tag{A.8}$$

4. Calculation of the operator $\hat{L}(x)$.

Here, it is convenient to use the DWF in coordinate representation, i.e.

$$\hat{\Phi}(\mathbf{r}) = \frac{u(r)}{r\sqrt{2}} (\boldsymbol{\epsilon} \boldsymbol{\sigma}) - \frac{w(r)}{2r} \left[\frac{3(\mathbf{r} \boldsymbol{\epsilon})(\mathbf{r} \boldsymbol{\sigma})}{r^2} - (\boldsymbol{\epsilon} \boldsymbol{\sigma}) \right], \quad \hat{\Psi}(\mathbf{q}) = \int d^3 r e^{-i\mathbf{q}\mathbf{r}} \hat{\Phi}(\mathbf{r}), \tag{A.9}$$

where $\hat{\Psi}(\mathbf{q})$ is given by Eqs. (6). For the DWF's of Bonn [28] and Paris [29] potentials the s - and d -wave functions (u and w , respectively) were parametrized [28, 30] in the form

$$u(p) = \sum_i \frac{C_i}{p^2 + m_i^2}, \quad w(p) = \sum_i \frac{D_i}{p^2 + m_i^2} \quad \left(\sum_i C_i = \sum_i D_i = \sum_i D_i m_i^2 = \sum_i \frac{D_i}{m_i^2} = 0 \right),$$

$$u(r) = \sum_i \frac{C_i}{4\pi} e^{-m_i r}, \quad w(r) = \sum_i \frac{D_i}{4\pi} e^{-m_i r} \left(1 + \frac{3}{m_i r} + \frac{3}{m_i^2 r^2} \right), \quad (\text{A.10})$$

Calculating the integral $\hat{L}(x)$ (14), we transform the factors $\hat{\Psi}(\mathbf{q}+\mathbf{\Delta})$ and $(q^2+x-0)^{-1}$ into the \mathbf{r} -representation and obtain

$$\hat{L}(x) = 2 \int \frac{d^3 r}{r} e^{i\mathbf{\Delta} \cdot \mathbf{r} + \alpha r} \hat{\Phi}(\mathbf{r}), \quad \alpha = \begin{cases} -a & (x > 0) \\ ia & (x < 0) \end{cases}, \quad a = \sqrt{|x|}. \quad (\text{A.11})$$

Let us rewrite the operator $\hat{\Phi}(\mathbf{r})$ in Eqs. (A.9) as $\hat{\Phi}(\mathbf{r}) = \Phi_{ij} \varepsilon_i \sigma_j$, where ε_i is the i -th component of the deuteron polarization vector. Then, from Eq. (A.11), we arrive at the expressions

$$\hat{L}(x) = L_{ij} \varepsilon_i \sigma_j, \quad L_{ij} = A \delta_{ij} + B \left(\frac{3\Delta_i \Delta_j}{\Delta^2} - \delta_{ij} \right), \quad (\text{A.12})$$

$$A = \sqrt{2} \int \frac{d^3 r}{r^2} e^{i\mathbf{\Delta} \cdot \mathbf{r} + \alpha r} u(r) = 4\sqrt{2} \pi \int dr e^{\alpha r} u(r) j_0(r\Delta),$$

$$B = -\frac{1}{2} \int \frac{d^3 r}{r^2} e^{i\mathbf{\Delta} \cdot \mathbf{r} + \alpha r} w(r) \left(\frac{3(\mathbf{\Delta} \cdot \mathbf{r})^2}{r^2 \Delta^2} - 1 \right) = 4\pi \int dr e^{\alpha r} w(r) j_2(r\Delta).$$

Making use of the functions $u(r)$ and $w(r)$, given by Eqs. (A.10), we obtain

$$A = \sum_i \sqrt{2} C_i J(m_i, a, \Delta), \quad a = \sqrt{|x|}, \quad (\text{A.13})$$

$$B = \sum_i D_i \left[\frac{3(\Delta^2 + x - m_i^2)}{8m_i \Delta^2} + \frac{3(\Delta^2 + x - m_i^2)^2 + 4m_i^2 \Delta^2}{8m_i^2 \Delta^2} J(m_i, a, \Delta) \right],$$

where

$$J(m, a, \Delta) = \frac{1}{\Delta} \arctan \frac{\Delta}{m+a} \quad (x > 0),$$

$$J(m, a, \Delta) = \frac{1}{2\Delta} \left[\arctan \frac{a+\Delta}{m} - \arctan \frac{a-\Delta}{m} + \frac{i}{2} \ln \frac{m^2 + (a+\Delta)^2}{m^2 + (a-\Delta)^2} \right] \quad (x < 0).$$

5. Expressions for the integrals $F_{a,b,c,d}$ (18).

For the wave functions $u(r)$ and $w(r)$, given by Eqs. (A.10), one can calculate the

integrals $F_{a,b,c,d}$ (18) analytically, and we obtain

$$\begin{aligned}
F_a &= \sum_{ij} \frac{C_i C_j}{4\pi\Delta} A_{ij} \quad \left(A_{ij} \equiv \arctan \frac{\Delta}{m_i + m_j} \right), \\
F_b &= \sum_{ij} \frac{D_i D_j}{8\pi} \frac{3(x+y+\Delta^2)^2 - 4xy}{4xy\Delta} A_{ij} \quad (x = m_i^2, \quad y = m_j^2), \\
F_c &= - \sum_{ij} \frac{C_i D_j}{8\pi} \left[\frac{3x}{4m_j\Delta^2} + \frac{4y\Delta^2 + 3(x-y+\Delta^2)^2}{4y\Delta^3} \right] A_{ij}, \\
F_d &= \sum_{ij} \frac{D_i D_j}{8\pi} \frac{3(x+y+\Delta^2)[\Delta^4 - (x-y)^2] - 8xy\Delta^2}{8xy\Delta^3} A_{ij}.
\end{aligned} \tag{A.14}$$

6. Estimation of the Coulomb cross section σ_C

Here we estimate the pure Coulomb cross section of the reaction $K^+d \rightarrow K^+pn$ in nonrelativistic case. With the s -wave DWF $u(p)$, we can write

$$\sigma_C = \int \frac{d^3\mathbf{p}}{(2\pi)^3} u^2(p) \int d\Omega |f_c|^2, \quad f_c = \frac{2\alpha_c \mu}{t}. \tag{A.15}$$

Where \mathbf{p} is the neutron-spectator 3-momentum in the deuteron rest frame; f_c is the Born amplitude of the Coulomb K^+p scattering; $d\Omega = dzd\varphi$ is the solid angle element in the final K^+p system; $\alpha_c \approx 1/137$; $\mu = m_K m/(m+m_K)$ is the reduced mass; and t is the four-momentum transfer squared. In the nonrelativistic form $t = -(\mathbf{q}_1 - \mathbf{q})^2$, where \mathbf{q}_1 (\mathbf{q}) is the initial (final) relative 3-momentum in the subprocess $K^+p_1 \rightarrow K^+p$ and p_1 is the virtual proton with the mass $m_1 \neq m$.

For the angular part of the integral $\int d\Omega |f_c|^2$, making use of the relations

$$q_1^2 - q^2 = 2\mu(m - m_1), \quad m_1 = m - \frac{p^2 + \alpha^2}{m}, \quad \alpha^2 = m\varepsilon_d,$$

where ε_d is the deuteron binding energy, we obtain

$$\int d\Omega |f_c|^2 = \frac{4\pi\alpha_c^2 m^2}{(p^2 + \alpha^2)^2} \tag{A.16}$$

We shall estimate the cross section σ_C (A.15) with the DWF of the simplest form $u(p) = \sqrt{8\pi\alpha}/(p^2 + \alpha^2)$. Formally, the integral $\int d^3\mathbf{p}$ (A.15) depends on the kinematical boundaries through the condition $\sqrt{s_{K^+p}} > m + m_K$, but we shall calculate it in the range $0 < p < \infty$. In this approximation it is supposed that the DWF is a rapid function of p and the process $K^+d \rightarrow K^+pn$ is considered in the region not very close to the threshold. However, we take into account the p -dependent factor (A.16). Finally, we obtain

$$\sigma_C = 16\alpha_c^2 \alpha m^2 \int_0^\infty \frac{p^2 dp}{(p^2 + \alpha^2)^4} = \frac{\pi \alpha_c^2}{2\varepsilon_d^2} \approx 6.5 \text{ mb.} \tag{A.17}$$

This value is not very small in comparison with the hadronic $K^+d \rightarrow K^+pn$ cross section, shown in Fig. 4a. We neglect the Coulomb contribution, since it is concentrated in the region of small scattering angles, which may be not accepted by the detectors.

References

- [1] T. Nakano *et al.*, (LEPS Collaboration), Phys. Rev. Lett. **91**, 012002 (2003); V.V. Barmin *et al.*, (DIANA Collaboration), Phys. At. Nucl. **66**, 1715 (2003); S. Stepanyan *et al.*, (CLAS Collaboration), Phys. Rev. Lett. **91**, 252001 (2003). See the full list of experimental evidence for and against the existence of the pentaquark Θ^+ in the recent review paper: M. Danilov and R. Mizuk, e-print arXiv: 0704.3531v1 [hep-ex] 26 April 2007.
- [2] R.A. Arndt, I.I. Strakovsky, and R.L. Workman, Phys. Rev. C **68**, 042201 (2003); Phys. Rev. C **69**, 019901 (2004) [nucl-th/0308012].
- [3] J. Haidenbauer and G. Krein, Phys. Rev. C **68**, 052201 (2003) [hep-ph/0309243].
- [4] S. Nussinov, hep-ph/0307357.
- [5] W.R. Gibbs, Phys. Rev. C **70**, 045208 (2004) [nucl-th/0405024].
- [6] R.N. Cahn and G.H. Trilling, Phys. Rev. D **69**, 011501 (2004) [hep-ph/0311245].
- [7] A. Sibirtsev, J. Haidenbauer, S. Krewald, and Ulf-G. Meißner, Phys. Lett. **599B**, 230 (2004) [hep-ph/0405099].
- [8] W.R. Gibbs and R. Arceo, nucl-th/0611095.
- [9] A. Sibirtsev, J. Haidenbauer, S. Krewald, and Ulf-G. Meißner, nucl-th/0608028.
- [10] T. Bowen *et al.*, Phys. Rev. D **2**, 2599 (1970).
- [11] T. Bowen *et al.*, Phys. Rev. D **7**, 22 (1973).
- [12] D.V. Bugg *et al.*, Phys. Rev. **168**, 1466 (1968).
- [13] A.S. Carrol *et al.*, Phys. Lett. **45B**, 531 (1973).
- [14] R.A. Burnstein *et al.*, Phys. Rev. D **10**, 2767 (1974).
- [15] T.F. Kycia *et al.*, Phys. Rev. **118**, 553 (1960).
- [16] C.J. Adams *et al.*, Phys. Rev. D **4**, 2637 (1971).
- [17] C.J. Adams *et al.*, Nucl. Phys. **B66**, 36 (1973).
- [18] W. Cameron *et al.*, Nucl. Phys. **B78**, 93 (1974).

- [19] V. Cook *et al.*, Phys. Rev. Lett. **7**, 182 (1961).
- [20] R.L. Cool *et al.*, Phys. Rev. D **1**, 1887 (1970).
- [21] G. Giacomelli *et al.*, Nucl. Phys. **B37**, 577 (1972).
- [22] V. E. Tarasov, V. V. Baru, and A. E. Kudryavtsev, Yad. Fiz. **63**, 871 (2000) [Phys. At. Nucl. **63**, 801 (2000)].
- [23] V.J. Stenger *et al.*, Phys. Rev. **134**, B1111 (1964).
- [24] A.B. Migdal, Sov. Phys. JETP **1**, 2 (1955).
- [25] K.M. Watson, Phys. Rev. **88**, 1163 (1952).
- [26] V.M. Kolybasov and V.G. Ksenzov, Yad. Fiz. **22**, 720 (1975) [Sov.J.Nucl.Phys. **22**, 372 (1975)].
- [27] L.D. Landau and E.M. Lifshitz. "Quantum Mechanics. Nonrelativistic Theory". ("Theoretical Physics", vol. III, Nauka, Moscow, 1989), p.641.
- [28] R. Machleidt *et al.*, Phys. Rep. **149**, 1 (1987).
- [29] M. Lacombe *et al.*, Phys. Rev. C **21**, 861 (1981).
- [30] M. Lacombe *et al.*, Phys. Lett. B **101**, 139 (1981).
- [31] S.S. Kamalov, J.A. Oller, E. Oset, and M.J. Vicente-Vacas, Phys. Rev. C **55**, 2985 (1997).
- [32] G. Giacomelli *et al.*, Nucl. Phys. **B68**, 285 (1974).
- [33] R.G. Glasser *et al.*, Phys. Rev. D **15**, 1200 (1977).
- [34] C.J.S. Damerell *et al.*, Nucl. Phys. **B94**, 374 (1975).
- [35] M. Sakitt *et al.*, Phys. Rev. D **15**, 1846 (1976).
- [36] W. Slater *et al.*, Phys. Rev. Lett. **7**, 378 (1961).
- [37] M. Sakitt *et al.*, Phys. Rev. D **12**, 3386 (1975).

Figure captions

- Fig. 1: The total K^+p (a), K^+n (b) and $K^+N(I=0)$ (c) cross sections. The curves correspond to different sets of the KN phase shifts (see text), and the symbols – to the experimental data. The filled (empty) symbols in Fig. 1a show the data on the total (elastic) K^+p cross sections.
- Fig. 2: The pole (M_1 and M_2) and the NN FSI (M_R) diagrams for the $Kd \rightarrow KNN$ process. The solid, dashed and double lines correspond to the kaons, nucleons and deuterons, respectively.
- Fig. 3: A single-scattering diagram for the elastic process $K^+d \rightarrow K^+d$. The lines of the particles are the same as in Fig. 2.
- Fig. 4: The total cross sections of the reactions $K^+d \rightarrow K^+pn$ (a) and $K^+d \rightarrow K^0pp$ (b). The symbols correspond to the experimental data (see references on the plot). The curves present the results of computations. Solid curves show the contributions of the amplitudes $M_1 + M_2 + M_R$ (Fig. a) and $M_1 + M_2$ (Fig. b); dashed-dotted curves – the results, obtained with the s -wave part of DWF; dashed curves "S" – the results, obtained with the s -wave KN amplitudes. The dashed and dotted curves in Fig. 4a show the contributions of the amplitudes $M_1 + M_2$ and M_R , respectively.
- Fig. 5: The K^+d total (a) and elastic (b) cross sections. The symbols correspond to the experimental data (see references on the plot). The curves show the results of computations. The total K^+d cross section (solid curve in Fig. 5a) is a sum of cross sections, shown by solid curves in Figs. 4a, 4b, and 5b. The dashed curve in Fig. 5a corresponds to the same sum but with contribution of the $K^+d \rightarrow K^+pn$ cross section (dashed curve in Fig. 4a), not corrected for NN FSI. The dashed-dotted curves show the results, obtained with the s -wave part of DWF.
- Fig. 6: Predictions for the K^+d cross sections at the beam momentum $p_{\text{LAB}} = 127 \text{ MeV}/c$ as the functions of the isoscalar KN scattering length a_0 . The plots show the $K^+d \rightarrow K^+pn$ (a), $K^+d \rightarrow K^0pp$ (b), K^+d total (c), and the elastic (d) cross sections. The curves 1 and 2 show the results for the values (taken from the Table) $a_1 = -0.328 \text{ fm}$ and $a_1 = -0.308 \text{ fm}$, respectively. The solid (dashed) curves in Figs. a, c show the results, obtained with (without) NN FSI correction to the $K^+d \rightarrow K^+pn$ cross section.

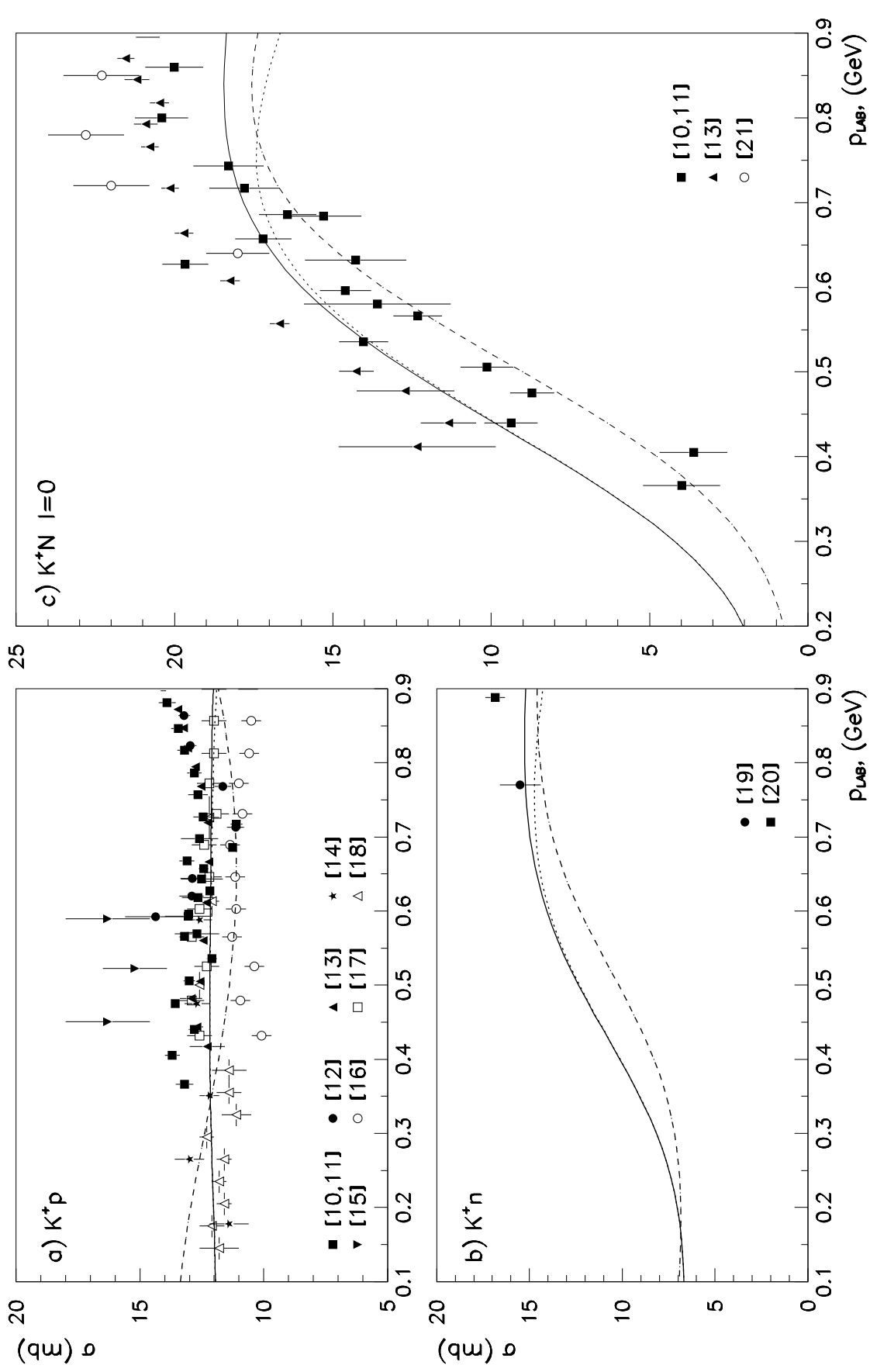


Fig. 1

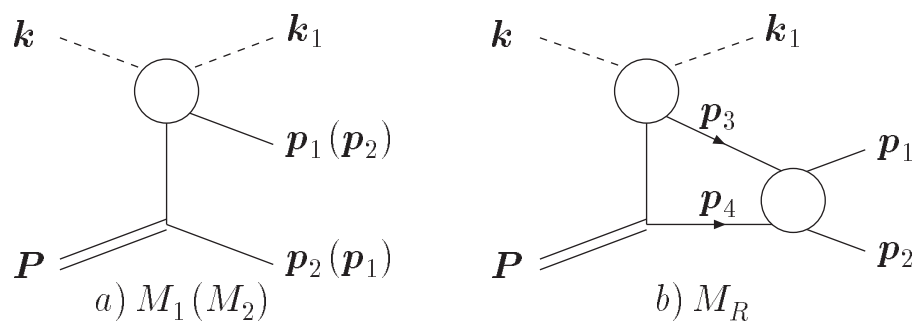


Fig. 2

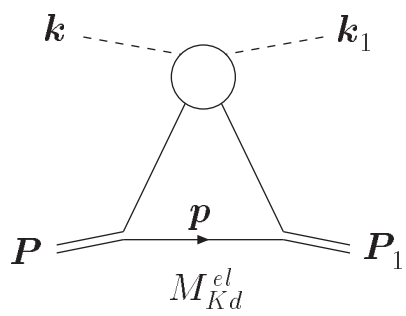


Fig. 3

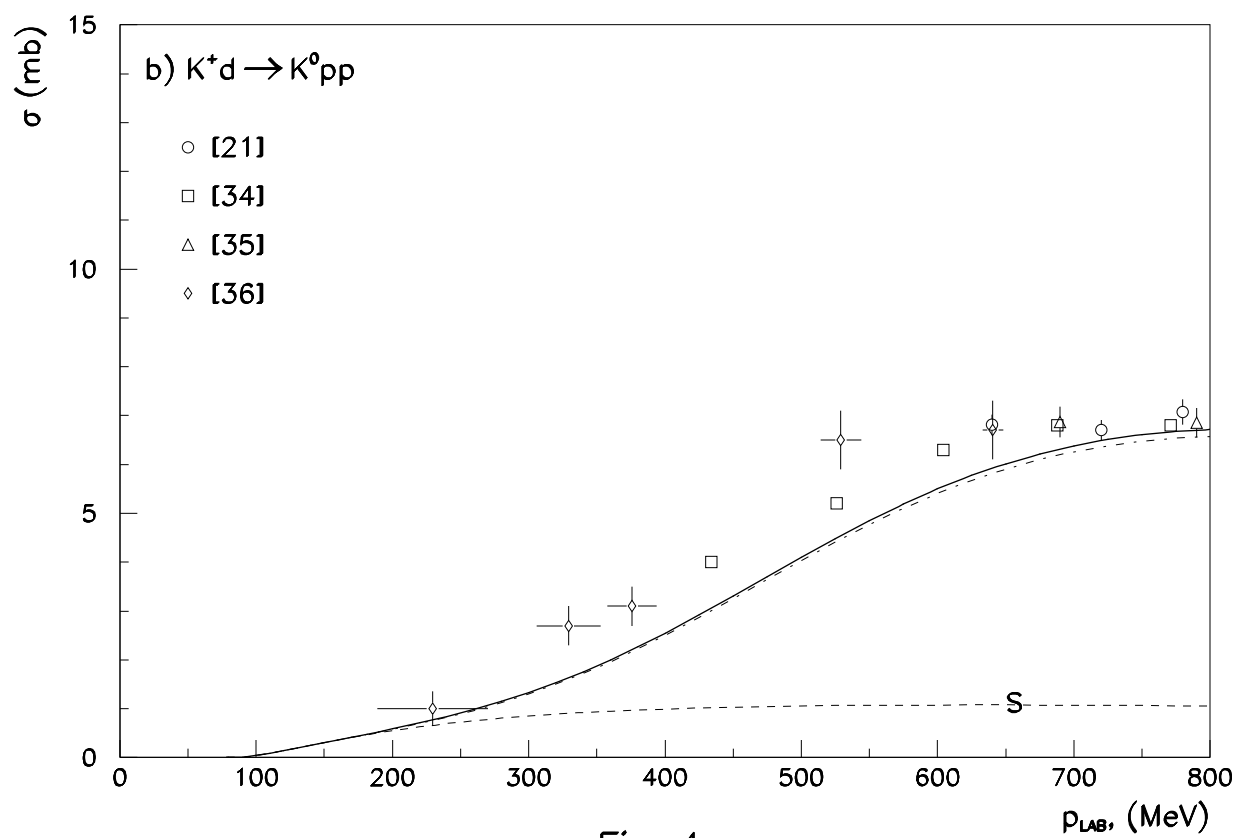
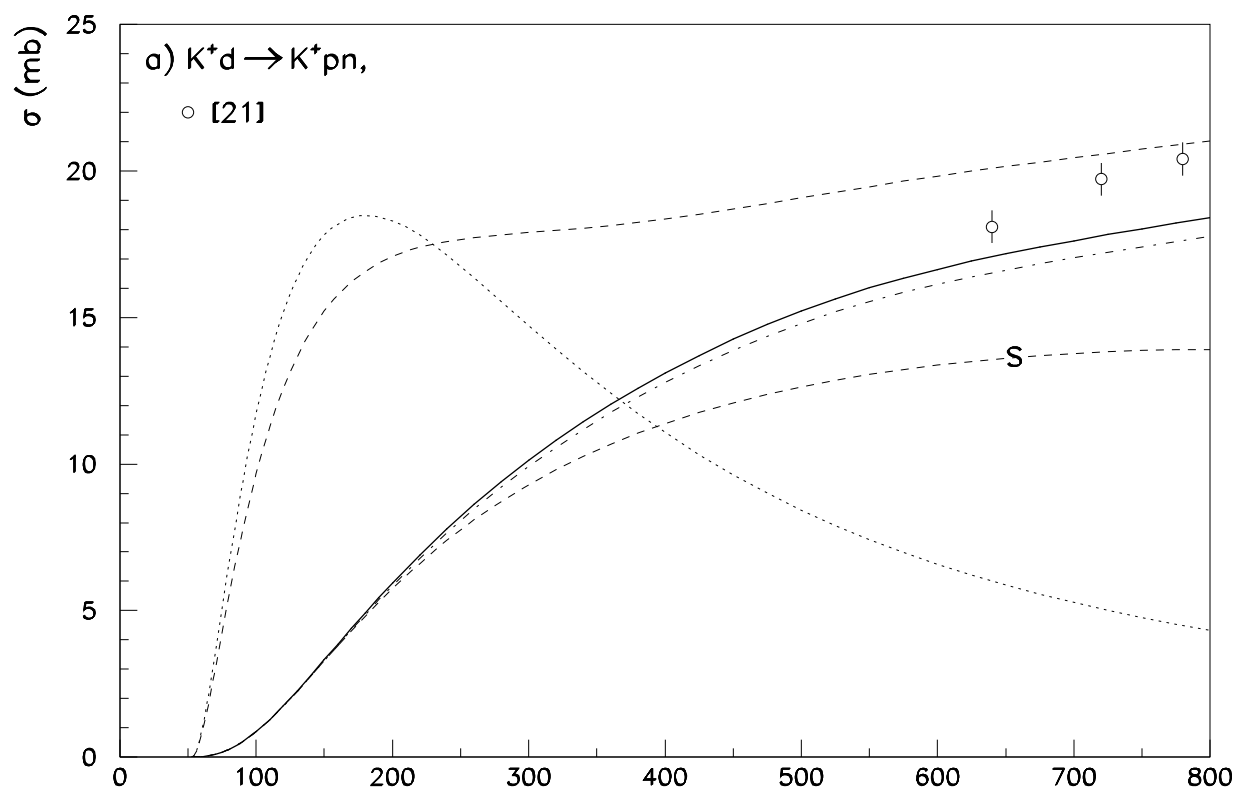
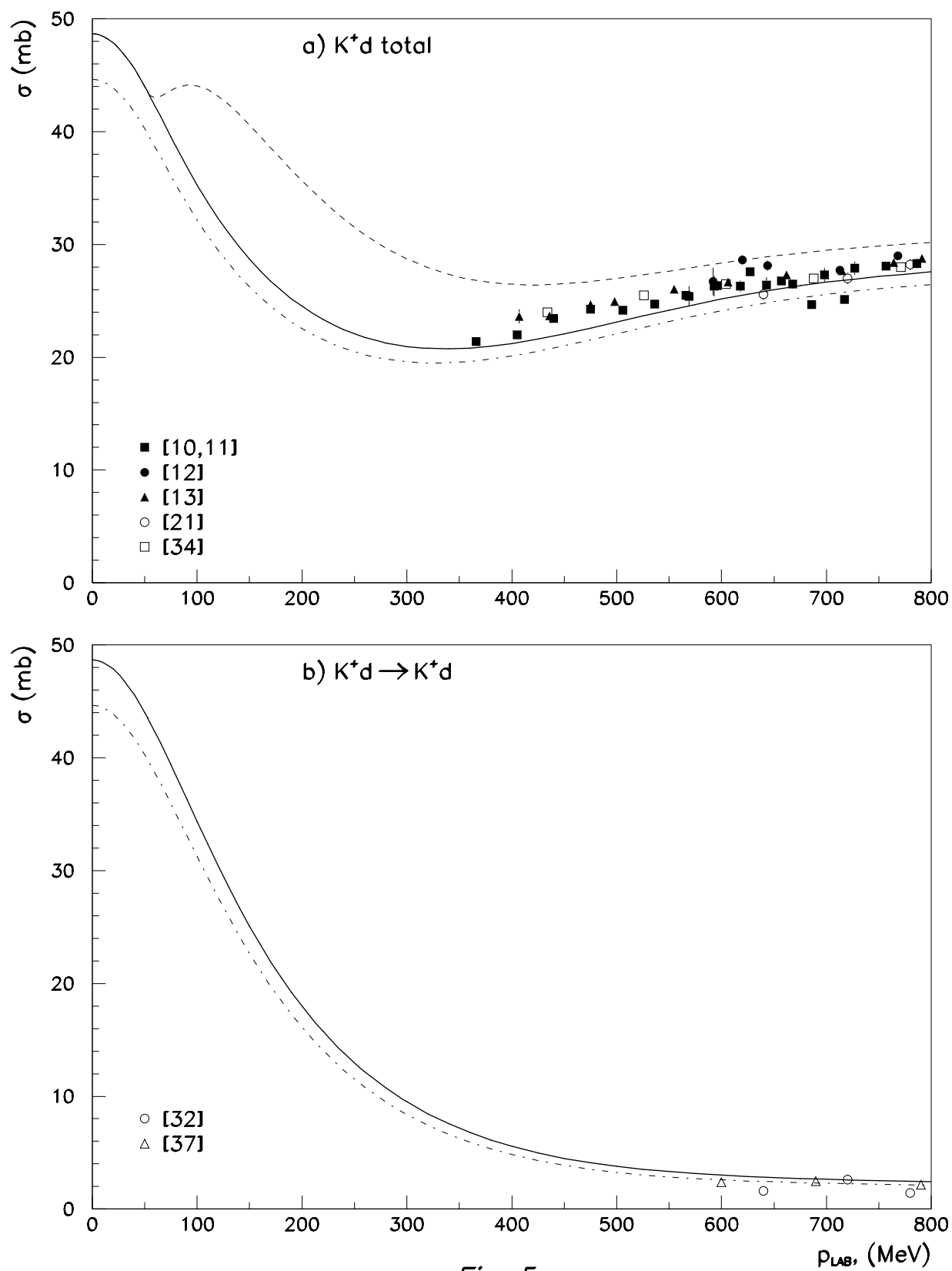


Fig. 4



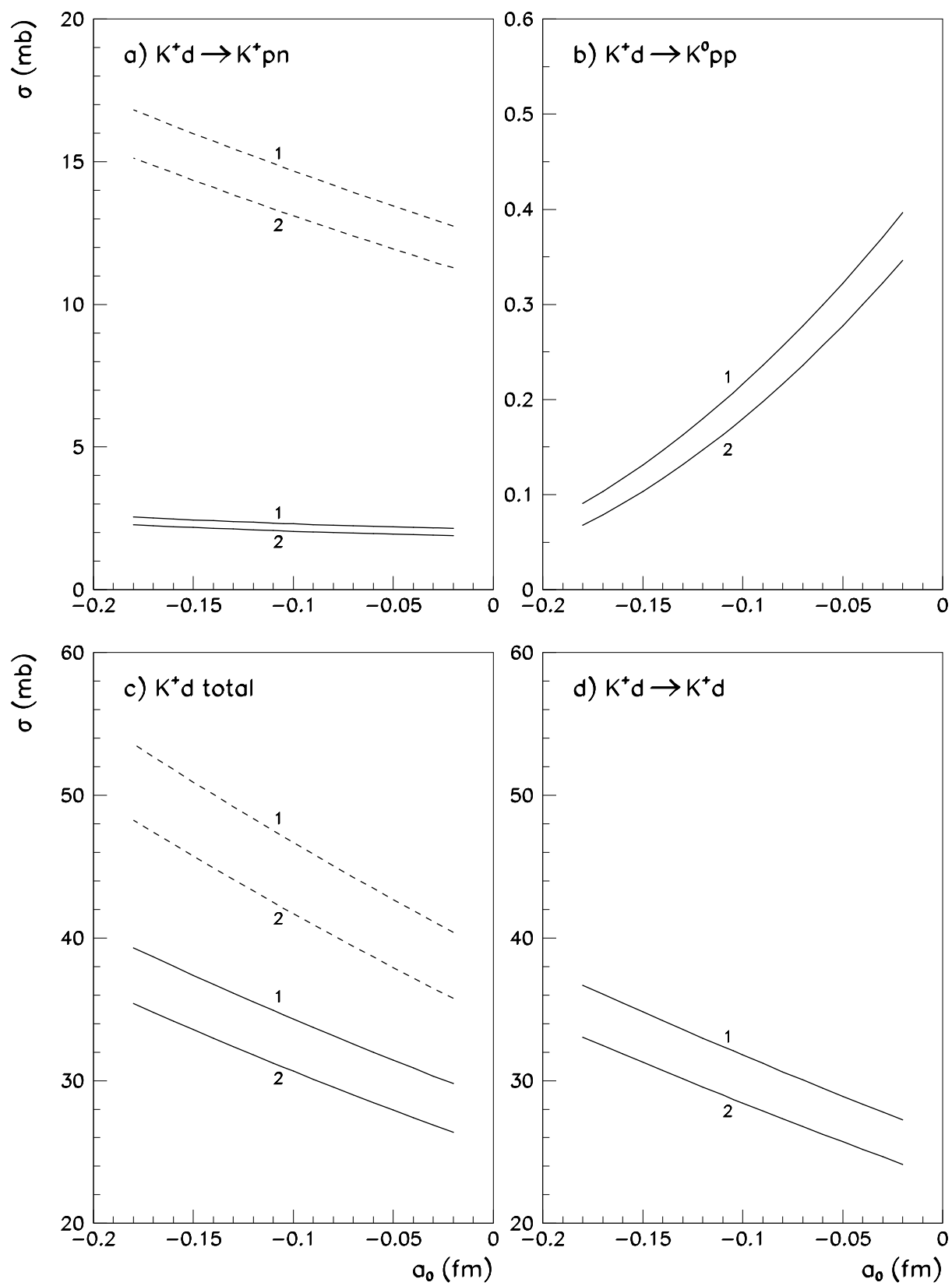


Fig. 6